On the Molecular Mechanisms of Elastin Coacervation and Coacervate Calcification

By Dan W. Urry

Laboratory of Molecular Biophysics and the Cardiovascular Research and Training Center,
University of Alabama Medical Center,
Birmingham, Alabama 35294

Received 5th December, 1975

Structural aspects and molecular details of the non-ionic simple coacervation of elastin peptide and water binary systems are considered from the viewpoint of the physical methods of proton and carbon-13 magnetic resonance, optical spectroscopy, high resolution electron microscopy and from the point of view of entropic aspects of inverse temperature transitions. Simple coacervation of tropoelastin is presented as the essential concentrating and aligning mechanism for elastogenesis. Scanning electron microscopy and electron probe microanalysis data from this laboratory are reviewed, which show that the non-ionic simple coacervates of α-elastin and tropoelastin serve throughout their bulk as matrices for the initiation of calcification.

The term coacervation was introduced by Bungenberg de Jong and Kruyt [1, 2] to describe an association of colloid particles which results in a colloid-rich liquid that does not exhibit the birefringence of a crystalline state. Coacervation is a reversible, concentration-dependent phase separation which may be elicited by changes in temperature, pH, salt concentrations, solvent compositions, or by addition of other macromolecules and which is observed as the incipient formation and coalescence of liquid droplets with greater density than the surrounding medium. The immediate effect is an increase in turbidity which in time dissipates through coalescence, with the formation of two transparent phases. The more dense phase is called the coacervate and the less dense phase is called the equilibrium solution.[3]

In the present endeavour, concern is with the molecular details of the coacervation process exhibited by elastin peptides and with properties of the elastin coacervates. A relatively simple binary system of elastin peptide and water exhibits a temperature-elicited coacervation. When observed by high resolution electron microscopy using the negative staining technique, the elastin coacervates are seen to have a filamentous appearance [4–6] with periodicities similar to those of native fibrous elastin examined in the same manner.[7] Coacervation of tropoelastin, the precursor protein of the fibrous core of the elastic fibre which contains interesting repeating peptide sequences [8] capable of independent coacervation,[6] has, therefore, been proposed to be the crucial concentrating and aligning process prior to covalent cross-linking.[5] As the temperature-elicited coacervation of elastin peptides results in a filamentous ordering of subunits which, at lower temperature, are molecularly dispersed in solution, this coacervation is an inverse temperature transition. As it is concentration dependent,[9] the implication at the molecular level is one of hydrophobic intermolecular association being the dominant process. This viewpoint is strongly reinforced by studies on a coacervatable synthetic high polymer of a tropoelastin repeat peptide which contains only three amino acids—valine, glycine, and proline. Stepwise synthesis and con-

formational analysis, using proton and carbon-13 magnetic resonance, of the repeat elastin peptides, results in conformational models for the synthetic high polymers of the repeat peptide sequences which, by their structure, demonstrate the dominance of hydrophobic intermolecular interactions.[10–12] Thus, whether one begins with the precursor protein or synthetic high polymers of the repeat peptides and studies the coacervation process leading to fibre formation,[4–6] or whether one begins with the elementary building blocks, the observed regular repeating peptides of tropoelastin,[8] and studies their solution conformation,[10–12] the conclusion is that the molecular process which is dominant in coacervation of elastin peptides is intermolecular hydrophobic side chain interaction.

Interest in the elastic fibre from a biomedical point of view derives from its role as the primary retractive force for extended ligaments and skin and for distended vascular wall and lung tissue and from the observation that the elastic fibre is a primary site of calcification and lipid deposition.[13] The nature of the coacervation (fibre forming) process, involving as it does intermolecular hydrophobic association, provides a rationale for lipid deposition, and elastin coacervates, having been shown to be excellent matrices for initiating calcification,[14–16] allow for the mechanism of at least one biological calcification to be detailed.[13, 17, 18]

SIMPLE COACERVATION EXEMPLIFIED BY BINARY SYSTEMS OF ELASTIN PEPTIDE AND WATER

Simple coacervation as defined by Bungenberg de Jong [3] is " concerned with non-ionised groups in the macromolecule " whereas complex coacervation was used for those coacervations involving " salt bonds ". The synthetic high polymers of the tropoelastin repeat peptides provide an informative set of macromolecules in that they allow stepwise insight into the molecular details of simple coacervation.

HIGH POLYMERS OF THE REPEAT PEPTIDES OF TROPOELASTIN

Three repeating peptide sequences have been reported to occur in tropoelastin.[8] They may be listed as a tetrapeptide $(Val_1\text{-}Pro_2\text{-}Gly_3\text{-}Gly_4)_n$, a pentapeptide $(Val_1\text{-}Pro_2\text{-}Gly_3\text{-}Val_4\text{-}Gly_5)_n$, and a hexapeptide $(Val_6\text{-}Ala_1\text{-}Pro_2\text{-}Gly_3\text{-}Val_4\text{-}Gly_5)_n$. An aqueous solution of the polytetrapeptide even at concentrations of 300 mg ml^{-1} and an n-value of about 40 does not coacervate in the temperature range 0 °C to 95 °C. It does, however, exhibit an interesting conformational change at 50 °C when studied by nuclear magnetic resonance.[12] What is observed in proton magnetic resonance is a decrease in the temperature coefficient of peptide NH chemical shifts, particularly of the Val_1 NH, at temperatures greater than 50 °C (see fig. 1 and table 1). We interpret the change to be an increase in shielding of the peptide NH as occurs with increased intramolecular hydrogen bonding. This increase in intramolecular order on increasing the temperature, i.e., this inverse temperature transition, is rationalized as a largely entropic process involving a trade in order between clathrate water surrounding exposed hydrophobic side chains and the polypeptide. The proposed process is schematically depicted in fig. 2A. On raising the temperature the amount of ordered, shell water decreases and the order of the peptide increases as correlative to hydrophobic side chain association.

The polypentapeptide, $HCO\text{-}(Val_1\text{-}Pro_2\text{-}Gly_3\text{-}Val_4\text{-}Gly_5)_n\text{-}Val\text{-}OMe$, differs structurally from the polytetrapeptide only by insertion of a valine between the two glycines. With this addition the high polymer undergoes a readily reversible coacervation which begins at about 30 °C. The molecules within the coacervate have a

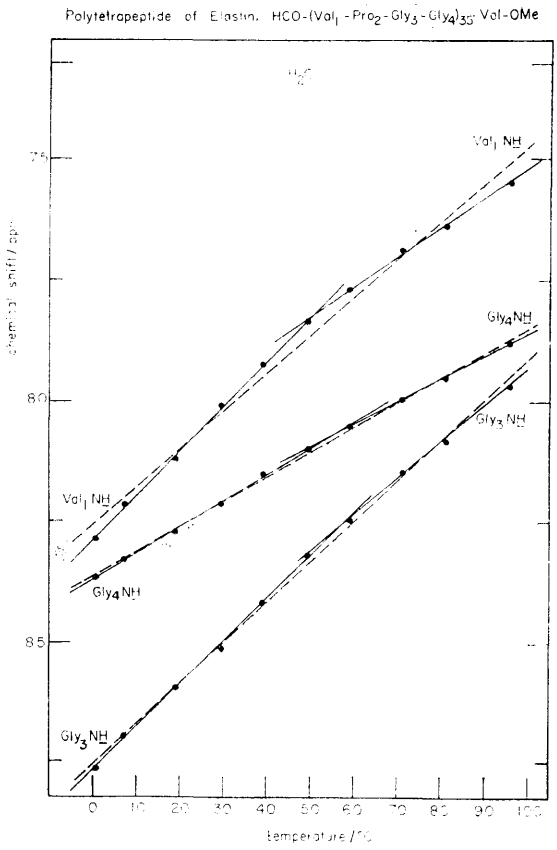

FIG. 1.—Temperature dependence of HCO-(Val_1-Pro_2-Gly_3-Gly_4)$_n$-Val-OMe peptide NH chemical shifts in water. Note that the Val_1 NH, in particular, exhibits a marked change in slope at 50 °C. This conformational change is indicative of increased order on raising the temperature. Adapted from Urry and Long.[12]

TABLE 1—TEMPERATURE DEPENDENCE OF PEPTIDE NH CHEMICAL SHIFTS ($d\delta/dT$)*

peptide residue	polytetrapeptide 0–50 °C	polytetrapeptide 50–100 °C	peptide residue	polypentapeptide 0–50 °C	polypentapeptide 50–100 °C	peptide residue	polyhexapeptide 0–50 °C	polyhexapeptide 50–100 °C
Val_1	−9.2	−6.2	Val_1	−9.2	−6.0			
						Ala_1	−9.3	−7.2
Pro_2			Pro_2			Pro_2		
Gly_3	−8.9	−7.6	Gly_3	−7.5	−6.1	Gly_3	+7.3	−5.5
			Val_4	−7.8	−5.5	Val_4	−7.0	−4.5
Gly_4	−5.5	−4.7	Gly_5	−8.2	−6.5	Gly_5	−7.2	−5.9
						Val_6	−7.3	−5.2

* Values given in ppm/deg times 10^3. From Urry and Long.[12]

substantial degree of mobility, since carbon-13 magnetic resonance spectra at 25 MHz can be obtained and the longitudinal relaxation times are of the order of 1 s for the carbonyl carbons and 0.1 s for the α-carbons. Interestingly, the equilibrium solution above the coacervate exhibits an intramolecular conformational change near 50 °C which is analogous to that exhibited by the polytetrapeptide. The temperature coefficients of chemical shift of polypentapeptide NH protons at concentrations less than

that of the equilibrium solution are included in table 1 where they may be compared with those of the polytetrapeptide. Therefore, at low concentrations the polypentapeptide exhibits the 50–60 °C transition as indicated in fig. 2A but, when there is sufficient concentration (>20 mg ml^{-1}), simple coacervation is observed at 30–40 °C as schematically represented in fig. 2B. Presumably with the greater ΔS which occurs

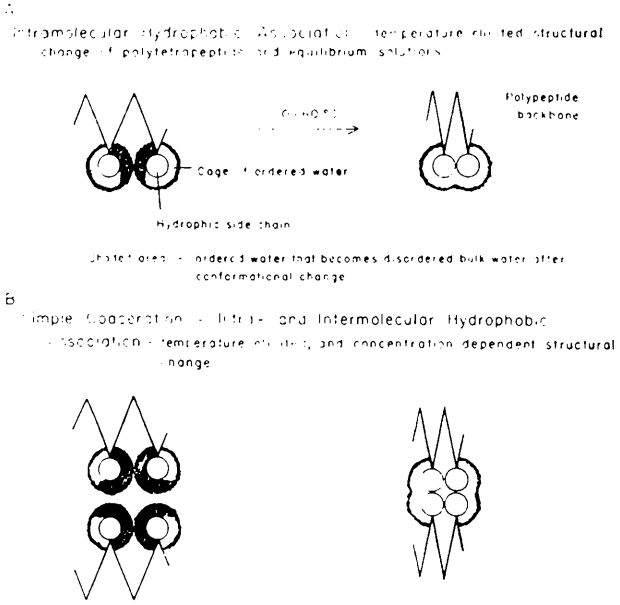

FIG. 2.—Schematic representation of (A) the intramolecular hydrophobic association aspect of the intramolecular conformational change of solutions of elastin peptides and (B) the intra- and intermolecular hydrophobic association attending simple coacervation of elastin peptides in water.

in the water part of the system on intermolecular association, the transition can occur at a lower temperature (30–40 °C) than when the ΔS (water) is less, as for an intramolecular hydrophobic association with the transition at higher temperature (i.e., 50–60 °C).

The polyhexapeptide, HCO-Val-(Ala$_1$-Pro$_2$-Gly$_3$-Val$_4$-Gly$_5$-Val$_6$)$_n$-OMe, in terms of primary structure differs from the polypentapeptide only by insertion of an Ala between the Val and Pro residues. At low concentrations, it exhibits the 50 °C conformational change seen with the polypenta- and polytetrapeptide (see table 1). At higher concentrations with an n-value of seven, the polyhexapeptide undergoes an essentially irreversible precipitation at about 80 °C. If, however, only one residue in 25 or 30 is made more hydrophobic by introduction of an aromatic group, a readily reversible coacervation occurs with the onset at about 20 °C. Carbon-13 magnetic resonance of this coacervate yields no spectrum even at 15 MHz, indicating a much decreased mobility over that of the polypentapeptide coacervate.

Summarizing the high polymer data, the polytetrapeptide does not coacervate but does exhibit a solution conformational change at 50 °C as do equilibrium solutions of the polypenta- and polyhexapeptides. The polypentapeptide coacervates with mobility observable in CMR at 15 and 25 MHz, and the polyhexapeptide precipitates, or with very slight modification coacervates, with no observable mobility at either 25 MHz or 15 MHz.

CONCENTRATION DEPENDENCE OF COACERVATION

Varying the temperature of a coacervatable solution and following the normalized turbidity results in a temperature profile for coacervation. Doing this for a series of concentrations readily demonstrates the concentration dependence of the process (see fig. 3A).[9] At high concentration, e.g., 40 mg ml^{-1}, the transition is almost vertical.

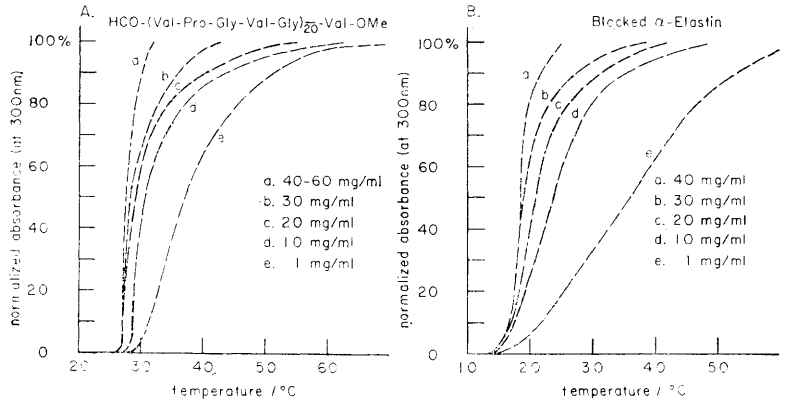

FIG. 3.—Concentration dependence of temperature profiles for simple coacervation of (A) the synthetic polypentapeptide of tropoelastin and (B) *N*-formylated and *O*-methylated *α*-elastin. From Urry, *et al.*[9]

As the concentration is decreased the transition occurs over a wider temperature range. This demonstrates the highly cooperative and intermolecular nature of the coacervation process. The amino acid composition of the polypentapeptide, and the apparent increase in order on raising the temperature,[6] define this coacervation process to be dominantly a process of intermolecular hydrophobic association (see fig. 2B).

α-Elastin, an approximately 70 000 dalton oxalic acid fragmentation product of fibrous elastin, contains on the average some sixteen peptide chains held together by four or five tetrasubstituted pyridinium cross-links each derived from four lysine side chains.[19–21] Depending on the fraction, *α*-elastin, which has been N-formylated and O-methylated to remove all charged groups, can exhibit a temperature profile which is virtually identical to that of the polypentapeptide with onset at about 30 °C, or a profile essentially similar to that of the coacervatable polyhexapeptide with onset between 10–20 °C as in fig. 3B.[9] This allows the conclusion that hydrophobic intermolecular interactions are dominant in the coacervation process.

MOLECULAR DETAILS OF COACERVATION

The schematic representation of elastin peptide coacervation given in fig. 2B is one of decreased order in the water part of the system, i.e., clathrate water → bulk water, and an increase in the order of the polypeptide The process should be viewed as dynamic average changes rather than as rigid changes in a specific site. With the results of extensive studies on the conformations of the repeat peptides of elastin,[12] it becomes possible to describe in considerable molecular detail the nature of the polypeptide conformations and the intra- and intermolecular interactions. The class of conformations that the polyhexapeptide and polypentapeptide represent are generic-

ally called β-spirals.[22] These are structures in which there is secondary structure within the repeating unit (dominated in these cases by a 10-atom hydrogen bonded ring termed a β-turn) and in which the repeating units are related by a helical or spiral symmetry operation.[22, 12]

The proposed secondary structure of the repeat pentapeptide is given in fig. 4 [23] where the hydrogen bonds are considered to be dynamic, with the probability of the Val_1 C–O . . . HN Val_4 hydrogen bond being of the order of 0.8 and that of the Gly_5 C–O . . . HN Gly_3 being about 0.6. The space filling model for a particular relationship between repeating units is given in fig. 5.[12] This β-spiral shows spiralling hydrophobic ridges comprised primarily of paired valyl side chains and spiralling hydrophilic ridges which are due to solvent exposed Pro_2 and Gly_3 carbonyl moieties. The paired valyl side chains are equivalent to the process shown in fig. 2A and the hydrophobic ridges provide for intermolecular hydrophobic association in a manner that can leave the resulting structure dynamic. Relaxation studies are in progress to obtain numerical values for the dynamics of both the polypeptide and water components of the coacervate.

COACERVATION AND BIOLOGICAL FIBRE FORMATION

CAN FIBROUS ELASTIN BE A RANDOM NETWORK?

Tropoelastin has a unique amino acid sequence rather than a non-determinable random amino acid sequence.[8] As the cross-links are derived from lysine residues, and as there are only about 40 lysine residues in the 800 amino acid tropoelastin molecule, the probability that a given residue is a potential for cross-linking is 40/800. This is to be contrasted with rubbers where every repeating unit is a potential cross-link. Now it has been concluded by one of the most outstanding schools of the properties of macromolecules that fibrous elastin, like rubbers, is unambiguously random, a cross-linked random network.[24] For a system of random tropoelastin molecules the probability that a contact between two molecules would involve a lysine in each chain, i.e., would provide a potential cross-link, would be $(40/800)^2$. The probability that a given chain would have twenty potential cross-linking contacts with a random system could be expressed as

$$(40/800)^2 \cdot (39/799)^2 \cdot (38/798)^2 \cdot (37/797)^2 \ldots (21/781)^2 \simeq 10^{-57}$$

that is, there is one chance in 10^{57} that a chain would have appropriate interchain contacts for 20 potential cross-links. Given a molecular correlation time of 80 ns as the time required to achieve each new configuration, it would take 10^{40} years for 10^{57} configurations, i.e., 10^{40} years for molecular system of random tropoelastin molecules to achieve 20 potential cross-links in which cross-linking would be achieved by two juxtaposed lysine residues. As nearly all of the 40 lysines become involved in cross-links, and as the cross-linking mechanism is more complex than the juxtapositioning of two lysine residues, it appears that there must be intermolecular ordering which assists in appropriate juxtapositioning of potential cross-linking residues. We suggest that the coacervation of tropoelastin provides the requisite intermolecular ordering [5] and that the system cannot be a random network of chains.[24]

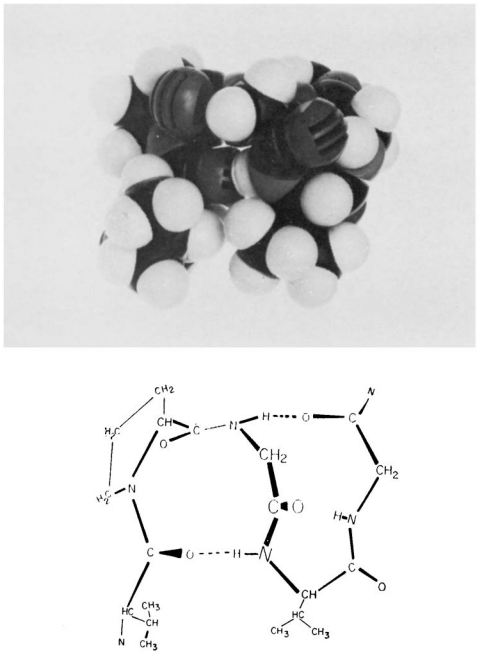

FIG. 4.—Proposed solution secondary structure of the repeat pentapeptide of tropoelastin. The probabilities of occurrence of the hydrogen bonds in water are approximately 0.8 for the 10-atom hydrogen bonded ring and 0.6 for the 11-atom hydrogen bonded ring. From Urry, *et al.*[10]

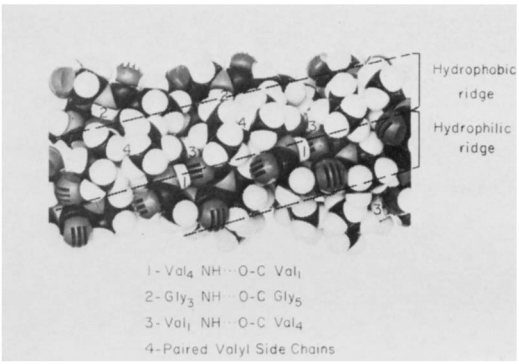

FIG. 5.—Working model for the coacervate conformation of the polypentapeptide of tropoelastin. There are three hydrogen bonds which are considered to occur with varying probability and there is a pair wise interaction between valyl side chains as a detailed example of the schematic representation of fig. 2A. The structure also contains spiralling hydrophobic ridges which are viewed as the bands giving rise to intermolecular hydrophobic association of simple coacervation as schematically represented in fig. 2B. Adapted from Urry and Long.[12]

[*To face page* 210

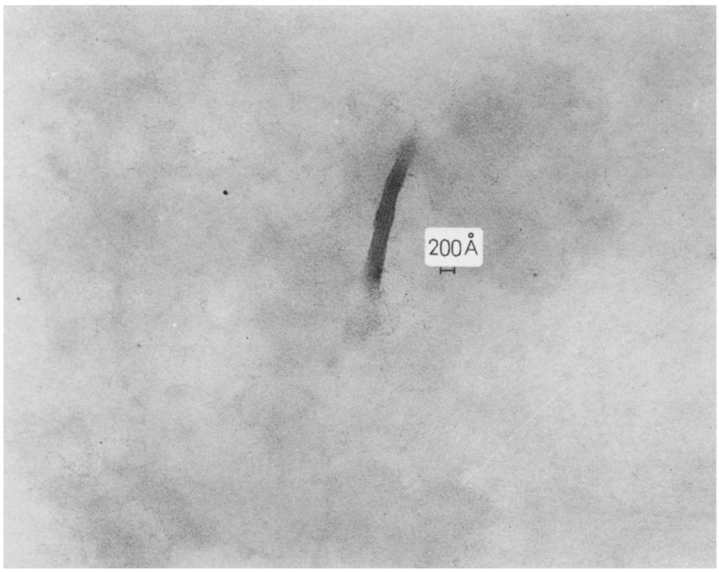

FIG. 6.—High resolution electron micrograph of negatively stained tropoelastin coacervate. Parallel aligned filaments are observed at 50 Å intervals. From Cox, *et al.*[5]

ELASTOGENESIS AND ELASTIN COACERVATES AS MODELS FOR FIBROUS ELASTIN

The elastin coacervates are the stable states of aqueous solutions of elastin peptides at body temperature; the elastin coacervates contain 60% water by volume, which is the same as for fibrous elastin,[25] and the elastin coacervates are filamentous (see fig. 6) with periodicities similar to those of fibrous elastin.[7] Not only can it be said that micrographs of negatively stained tropoelastin coacervate have localized filamentous areas with similar periodicities to that of similarly examined fibrous elastin, but optical diffraction of both give 50 Å equatorial reflections [26, 27] and the argument that the electron microscopy result is an artifact is dispelled with the finding that low angle X-ray diffraction studies on fibrous elastin gives the same 50 Å equatorial reflection.[28] Therefore, we argue that the elastin coacervates are useful models for fibrous elastin and that coacervation of tropoelastin is the crucial concentrating and aligning step of elastogenesis which is required to achieve proper cross-linking.

From the results of the approaches that we have used to study fibrous elastin, it is not amorphous, isotropic or random but rather we believe that there is an ordering of subunits into filamentous arrays and that there are elements of order within the subunits.

CALCIFICATION OF ELASTIN COACERVATES

Having discussed the properties of elastin coacervates and argued that the coacervation process is the mechanism of elastic fibre formation, it is of added interest that these coacervates have been shown to be excellent matrices for the initiation of calcification [14–16] and, because of their relative molecular simplicity, calcification of elastin coacervates allows for a more detailed understanding of the mechanism of calcification.

In 1971 [17] we proposed that the essential elements of the Ca^{++} binding site for the initiation of calcification of elastic fibres were the peptide carbonyls of glycine-containing peptide sequences and that negatively charged groups were not essential to selective binding of Ca^{++} for the initiation of calcification. Briefly the mechanism was one of neutral site binding of Ca^{++} followed by charge neutralization by multivalent anions.

This mechanism of calcification which utilizes the carbonyls of glycine-containing peptide sequences was proposed before the repeat sequences of tropoelastin were found.[8] The repeat peptides of elastin have been synthesized in this laboratory and found selectively to bind Ca^{++} with affinity constants as high as 10^6.[29, 30] Furthermore a working model of the hexapeptide-Ca^{++} complex has been derived [31] which lends itself to detailing further the steps of fibrous elastin calcification.[13]

For lack of space, major conclusions of our elastin coacervate calcification studies will only be summarized. α-Elastin and tropoelastin coacervates and fibrous elastin are excellent calcifying matrices with either barbital buffer or serum media.[14, 15] The finding that tropoelastin calcifies demonstrates that it is not necessary that the chains be held together by covalent bridging, and that desmosine and isodesmosine cross-links are not necessary components of an initiation site.[15] Calcification of α-elastin and tropoelastin coacervates after pretreatment by chemical blocking of the amino and carboxylate groups provides verification of the neutral site mechanism for the initiation of calcification.[14, 15, 17] The rate of calcification is faster when the coacervate is formed under conditions which optimize intermolecular order.[15] Scanning electron microscopy studies verify coacervate calcification and electron probe microanalysis

(see fig. 7 and 8) shows calcification to be uniform over the surface of the coacervate to about a resolution of 1μm.[16] An additional crucial point is whether the calcification is a surface phenomenon, limited to the surface layer of the coacervate, or whether it penetrates into the coacervate. SEM and electron probe microanalysis of Araldite embedded, 0.5μm cross-sections of calcified coacervate demonstrate that calcification, while heavier near the surface, penetrates throughout the 10μm depth of the coacervate (see fig. 8).

This work was supported by National Institutes of Health Grant HL-11310. The author gratefully acknowledges the support and contributions of the many past and present members of the Laboratory of Molecular Biophysics.

[1] H. G. Bungenberg de Jong and H. R. Kruyt, *Proc. Kon. Ned. Akad. Wet.*, 1929, **32,** 849.
[2] H. G. Bungenberg de Jong and H. R. Kruyt, *Kolloid-Z.*, 1930, **50,** 39.
[3] H. G. Bungenberg de Jong, *Colloid Sci.*, ed. H. R. Kruyt (Elsevier, Amsterdam, 1949), vol. 2, chap. VIII, p. 232.
[4] B. A. Cox, B. C. Starcher and D. W. Urry, *Biochim. Biophys. Acta*, 1973, **317,** 209.
[5] B. A. Cox, B. C. Starcher and D. W. Urry, *J. Biol. Chem.*, 1974, **249,** 997.
[6] D. W. Urry, M. M. Long, B. A. Cox, T. Ohnishi, L. W. Mitchell and M. Jacobs, *Biochim. Biophys. Acta*, 1974, **371,** 597.
[7] L. Gotte, M. G. Giro, D. Volpin and R. W. Horne, *J. Ultrastruct. Res.*, 1974, **46,** 23.
[8] J. A. Foster, E. Bruenger, W. R. Gray and L. B. Sandberg, *J. Biol. Chem.*, 1973, **248,** 2876.
[9] D. W. Urry, M. M. Long, D. W. Mason and M. A. Jacobs, *Int. Res. Comm. Syst.*, 1975, **3,** 572.
[10] D. W. Urry, L. W. Mitchell, T. Ohnishi and M. M. Long, *J. Mol. Biol.*, 1975, **96,** 101.
[11] D. W. Urry, T. Ohnishi, M. M. Long and L. W. Mitchell, *Int. J. Pept. Protein Res.*, 1975, **7,** 367.
[12] D. W. Urry and M. M. Long, *CRC Crit. Rev. Biochem.*, 1976, in press.
[13] D. W. Urry, *Perspect. Biol. Med.*, 1974, **18,** 68.
[14] B. C. Starcher and D. W. Urry, *Biochem. Biophys. Res. Comm.*, 1973, **53,** 210.
[15] B. C. Starcher, B. A. Cox and D. W. Urry, *Calcif. Tiss. Res.*, 1974, **17,** 1.
[16] B. A. Cox, B. C. Starcher and D. W. Urry, *Calcif. Tiss. Res.*, 1975, **17,** 219.
[17] D. W. Urry, *Proc. Nat. Acad. Sci. USA*, 1971, **68,** 810.
[18] D. W. Urry, *Adv. Exp. Med. Biol.*, 1974, **43,** 211.
[19] S. M. Partridge, H. F. Davis and G. S. Adair, *Biochem. J.*, 1955, **61,** 11.
[20] S. M. Partridge and H. F. Davis, *Biochem. J.*, 1955, **61,** 21.
[21] S. M. Partridge, *Gerontologia*, 1969, **18,** 85.
[22] D. W. Urry, *Proc. Nat. Acad. Sci. USA*, 1972, **69,** 1610.
[23] D. W. Urry, L. W. Mitchell, T. Ohnishi and M. M. Long, *J. Mol. Biol.*, 1975, **96,** 101.
[24] S. R. Kakivaya and C. A. J. Hoeve, *Proc. Nat. Acad. Sci. USA*, 1975, **72,** 3505.
[25] S. M. Partridge, *Biochim. Biophys. Acta*, 1967, **140,** 132.
[26] L. Gotte, D. Volpin, R. W. Horne and M. Mammi, *Micron*, 1976, in press.
[27] D. Volpin, D. W. Urry, B. A. Cox and L. Gotte, (in preparation).
[28] A. Serafini-Fracassini, J. M. Field, M. Spina, W. G. S. Stephens and B. Delf, *J. Mol. Biol.* 1976, in press.
[29] D. W. Urry, W. D. Cunningham and T. Ohnishi, *Biochim. Biophys. Acta*, 1973, **291,** 853.
[30] M. M. Long, T. Ohnishi and D. W. Urry, *Arch. Biochem. Biophys.*, 1975, **166,** 187.
[31] D. W. Urry and T. Ohnishi, *Bioinorg. Chem.*, 1974, **3,** 305.
[32] D. W. Urry, C. F. Hendrix and M. M. Long, *Calcif. Tiss. Res.*, 1976, in press.

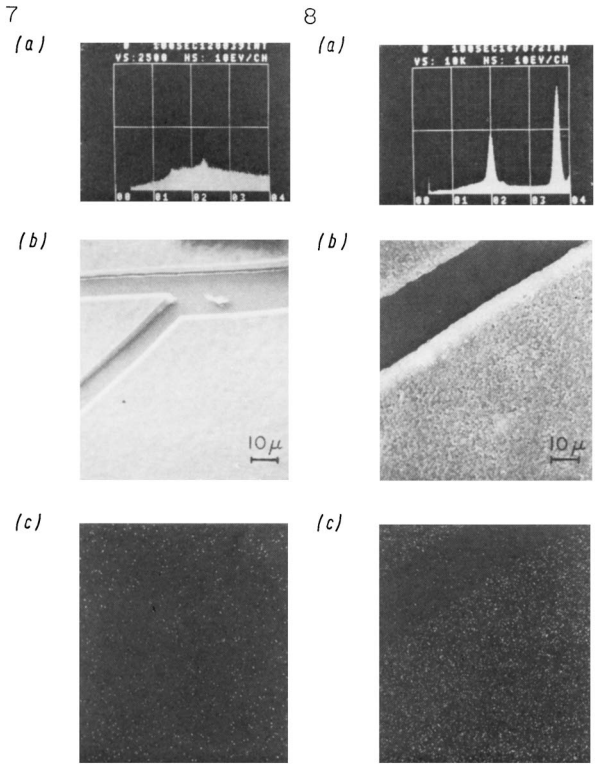

FIG. 7.—α-Elastin coacervate on a Plexiglas substrate. *a*—energy dispersive X-ray spectrum; *b*—scanning electron micrograph; *c*—elemental map for calcium distribution. Note that there is no difference between the coacervate and the cracks in the coacervate which expose the Plexiglas support. From Cox, *et al.*[16]

FIG. 8.—Serum calcified α-elastin coacervate on a Plexiglas support. *a*—Energy dispersive X-ray spectrum showing phosphorus and calcium peaks; *b*—scanning electron micrograph showing roughened surface of calcified coacervate; *c*—elemental map for calcium distribution. Contrast is seen between calcium in coacervate and lesser background counts over the exposed Plexiglas. From Cox, *et al.*[16]

[*To face page* 212

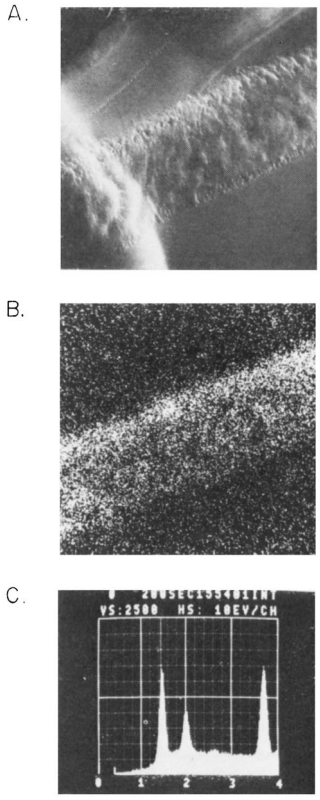

FIG. 9.—SEM and SEM microanalysis of 0.5 μm cross-sections of serum calcified coacervate. A. Energy dispersive X-ray spectrum. The lowest peak near 1.4 keV is the aluminium coating. The peak at 2.01 keV is due to the $K\alpha_{1,2}$ emissions of phosphorus, and the peak at 3.69 keV represents the $K\alpha_{1,2}$ X-rays of calcium. B. SEM micrograph of the cross-section of the 10 μm thick calcified coacervate embedded in Araldite. The same area from which the X-ray spectrum of A was obtained. C. Calcium distribution map of section in B which shows calcium heavier at the serum side of the coacervate but also penetrating the full depth of the coacervate. From Urry, *et al.*[32]